Journal of Geophysical Research: Planets

Supporting Information for

The chemostratigraphy of the Murray formation and role of diagenesis at Vera Rubin ridge in Gale crater, Mars, as observed by the ChemCam instrument

J. Frydenvang[1], N. Mangold[2], R.C. Wiens[3], A.A. Fraeman[4], L.A. Edgar[5], C. Fedo[6], J. L'Haridon[2], C.C. Bedford[7,8], S. Gupta[9], J.P. Grotzinger[10], J.C. Bridges[11], B.C. Clark[12], E.B. Rampe[8], O. Gasnault[13], S. Maurice[13], P.J. Gasda[3], N.L. Lanza[3], A.M. Olilla[3], P.-Y. Meslin[13], V. Payré[14], F. Calef[4], M. Salvatore[15], C.H. House[16]

[1]University of Copenhagen, Copenhagen, Denmark
[2]LPG, Université de Nantes, Nantes, France
[3]Los Alamos National Laboratory, Los Alamos, NM, USA
[4]Jet Propulsion Laboratory, California Institute of Technology, Pasadena, CA, USA
[5]U. S. Geological Survey, Flagstaff, Az, USA
[6]University of Tennessee, Knoxville, TN, USA
[7]Open University, Milton Keynes, UK
[8]NASA Johnson Space Center, Houston, TX, USA
[9]Imperial College, London, UK
[10]California Institute of Technology, Pasadena, CA, USA
[11]University of Leicester, Leicester, UK
[12]Space Science Institute, Littleton, CO, USA
[13]Institut de Recherche en Astrophysique et Planétologie, Université de Toulouse, CNRS, CNES, UPS, Toulouse, France
[14]Rice University, Houston, TX, USA
[15]Northern Arizona University, Flagstaff, AZ, USA
[16]Department of Geosciences and Earth and Environmental Systems Institute, Pennsylvania State University, The Pennsylvania State University, University Park, PA, USA

Contents of this file

Additional Supporting Information (Files uploaded separately)

Introduction

Included are three tables and nine figures to support the main manuscript. Table S1 includes all data used for the analysis and plots included in both the main manuscript and supporting figures. Importantly, table S1 includes the spacecraft clock for each ChemCam observation point that serves as a unique identifier that enable the full spectrum to be located and downloaded via the NASA PDS system (http://pds-geosciences.wustl.edu/missions/msl/). Table S2 adds to the information provided in table S1 by specifying all the

sub-classes ChemCam observation points have been assigned to since arriving at the Murray formation around sol 750 of the MSL mission. Table S3 provides the observed stratigraphic correlation coefficient matrix between each element/value included in this manuscript.

Figures S1-S9 provide additional context to the manuscript, including the location for each of the successful drill samples acquired as part of the VRR campaign (Figures S1 and S8), and not least the chemostratigraphy including the Marias Pass class (upper Pahrump Hills member) (Figures S2 and S3).

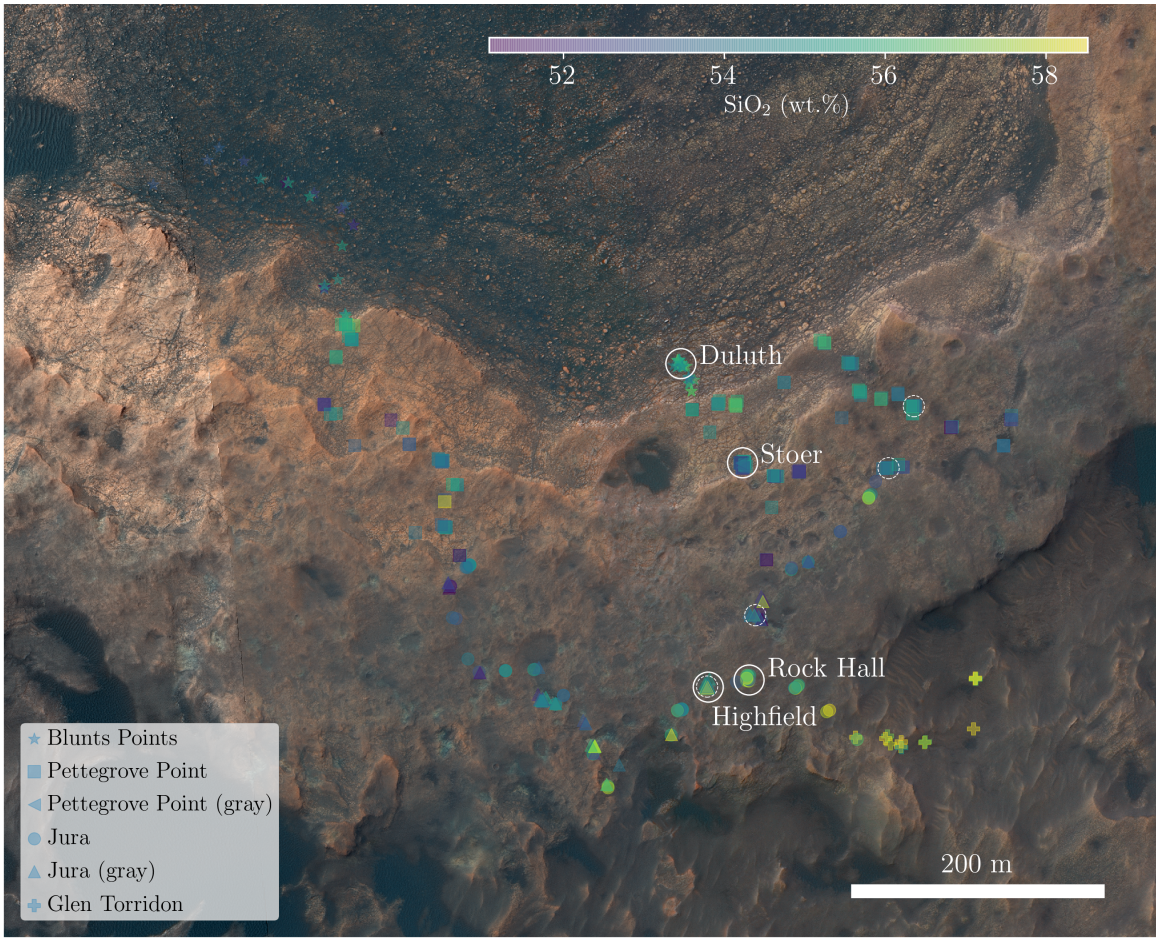

Figure S1. ChemCam observation points plotted on HiRISE mosaic showing the Vera Rubin ridge in Gale crater (Calef & Parker, 2016). Color code indicates the median SiO_2 content of points on bedrock targets in each ChemCam target acquired on the ridge. The location of the four drill sites on VRR is highlighted and named. The location of another four unsuccessful drill sites is annotated with dashed circles.

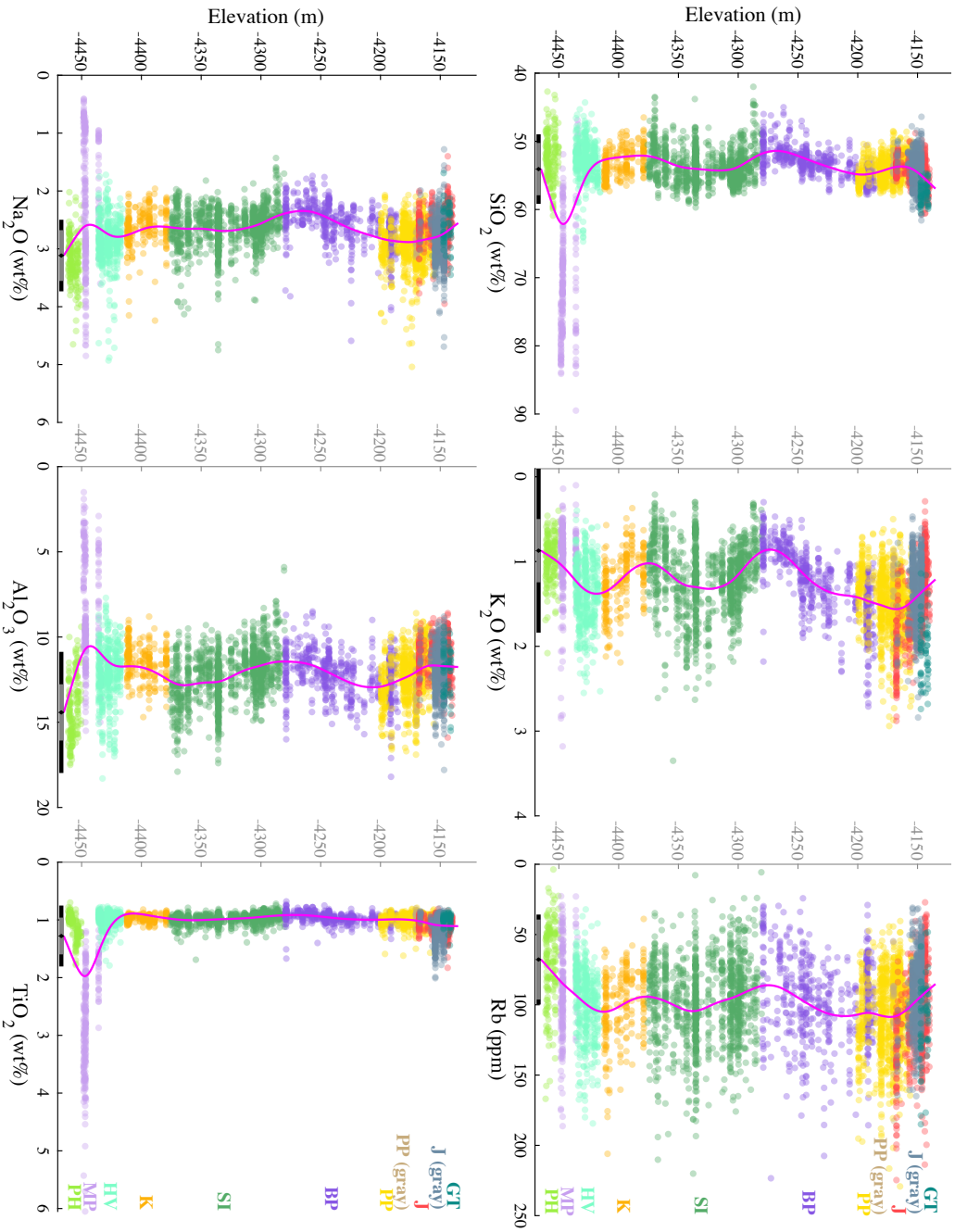

Figure S2. The geochemistry from individual ChemCam observation points against elevation for the oxides and elements: SiO_2, K_2O, Rb, Na_2O, Al_2O_3 and TiO_2. The black bar represents the mean absolute accuracy for all observation points as noted in Table S1; the gray bar represents the relative precision between Murray bedrock targets, see section 3.3 for details. The magenta line is a smoothing spline fitted to the data in each subplot. The annotated classes are: PH = Pahrump Hills, MP = Marias Pass, HV = Hartmann's Valley, K = Karasburg, SI = Sutton Island, BP = Blunts Point, PP = Pettegrove Point, J = Jura and GT = Glen Torridon. For J and PP, distinct classes of gray rocks are also annotated. Vera Rubin ridge comprises bedrock from the Pettegrove Point and Jura members.

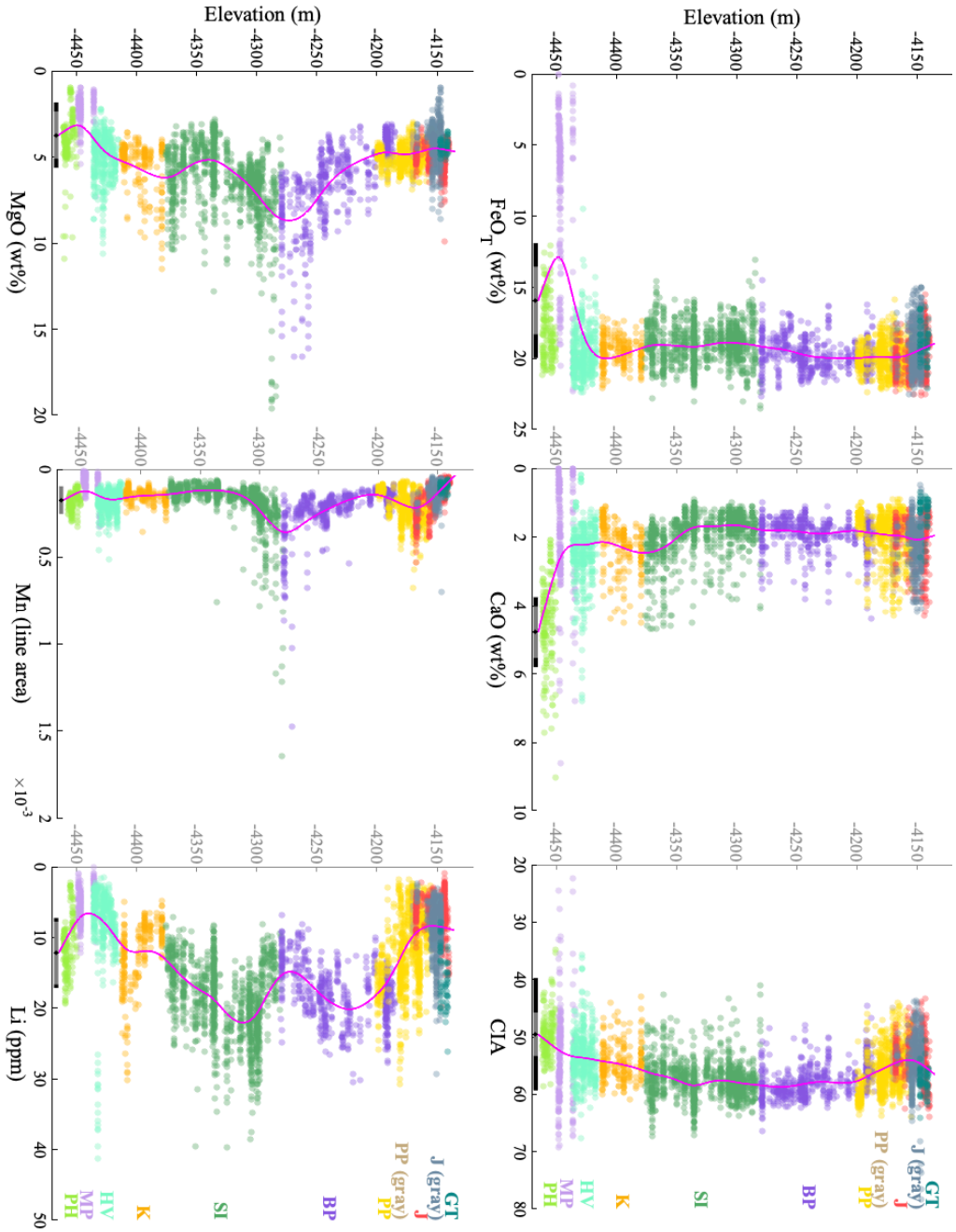

Figure S3. Plotting the geochemistry from individual ChemCam observation points against elevation for: FeO_T, CaO, MgO, MnO, Li and the Chemical Index of Alteration (CIA). The black bar represents the mean absolute accuracy for all observation points as noted in Table S1; the gray bar represents the relative precision between Murray bedrock targets, see section 3.3 for details. The magenta line is a smoothing spline fitted to the data in each subplot. The annotated classes are: PH = Pahrump Hills, MP = Marias Pass, HV = Hartmann's Valley, K = Karasburg, SI = Sutton Island, BP = Blunts Point, PP = Pettegrove Point, J = Jura and GT = Glen Torridon. For J and PP, distinct classes of gray rocks are also annotated. Vera Rubin ridge comprises bedrock from the Pettegrove Point and Jura members

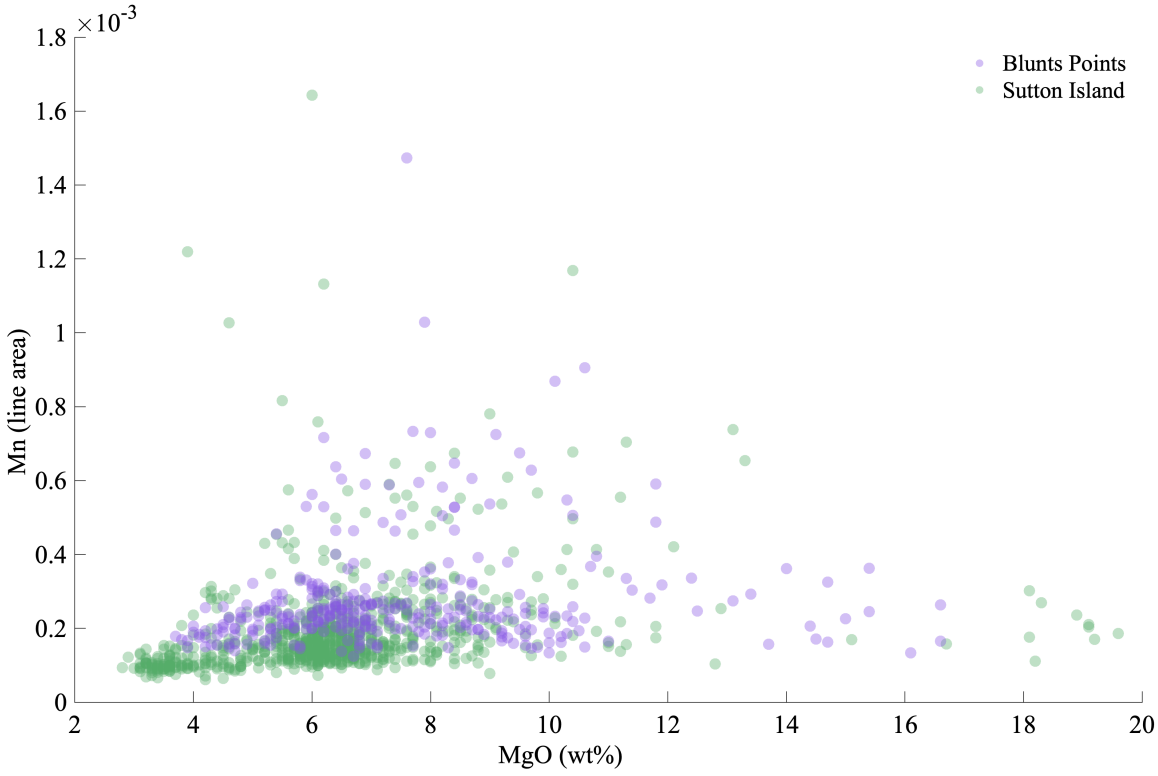

Figure S4. MgO and the normalized line intensity for Mn plotted against each other for the Blunts Point and Sutton Island member observations points at the member contact between elevation -4340 m to -4225 m. While both MgO and Mn show a notable increase at the contact between the Blunts Point and Sutton Island members (Figure 4), no apparent point-to-point correlation exist between these.

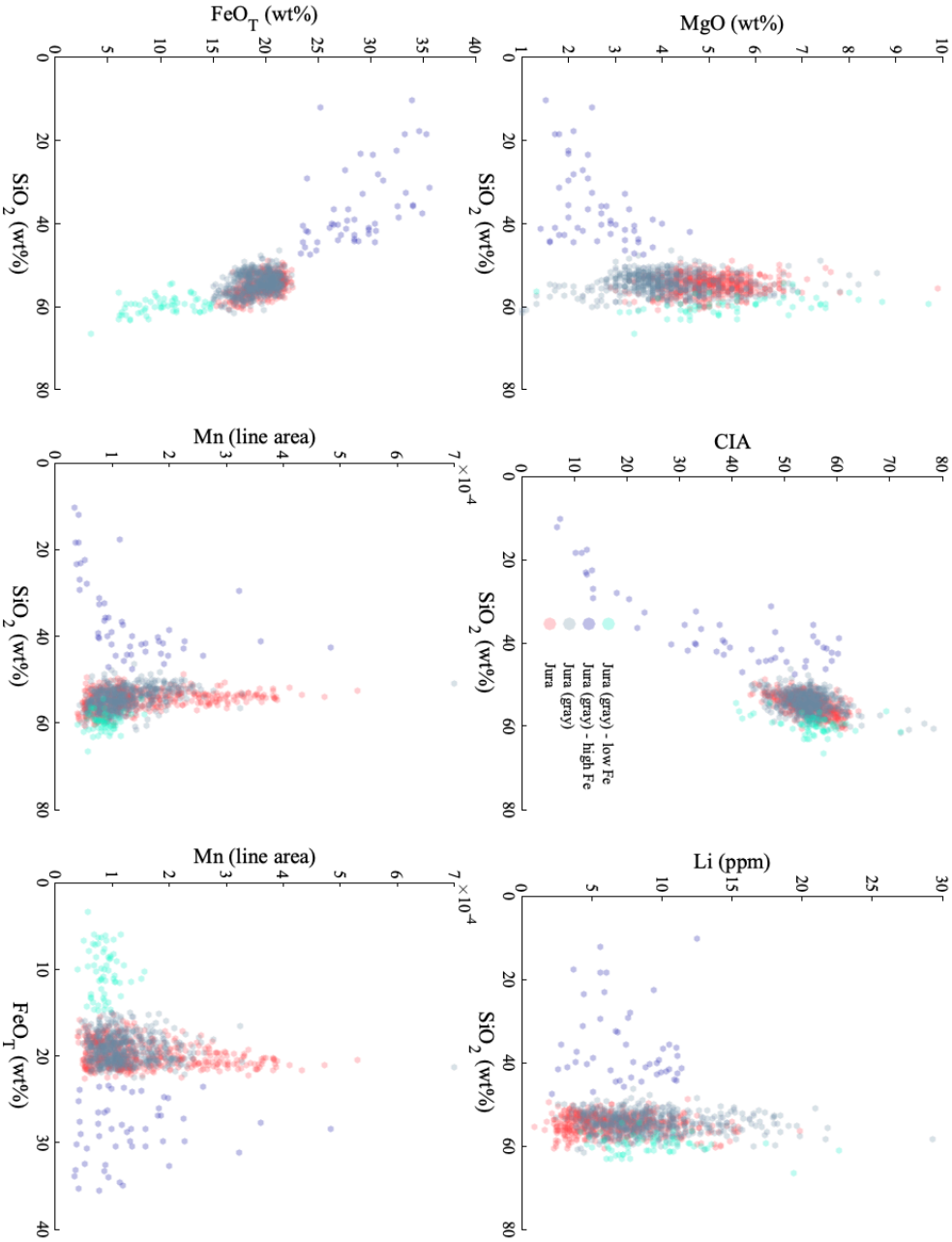

Figure S5. ChemCam observation points on red and gray Jura bedrock, as well as points in gray Jura identified as belonging to the either high or low Fe class. MgO, CIA, Li, FeO_T, and Mn (normalized line area) are plotted against SiO_2 abundance. Additionally, Mn (normalized line area) is plotted against FeO_T in lower right plot. High-Fe points exist with FeO_T abundance predicted above 36 wt.%, but these are not included here as they fall outside the predictive range of the ChemCam calibration model.

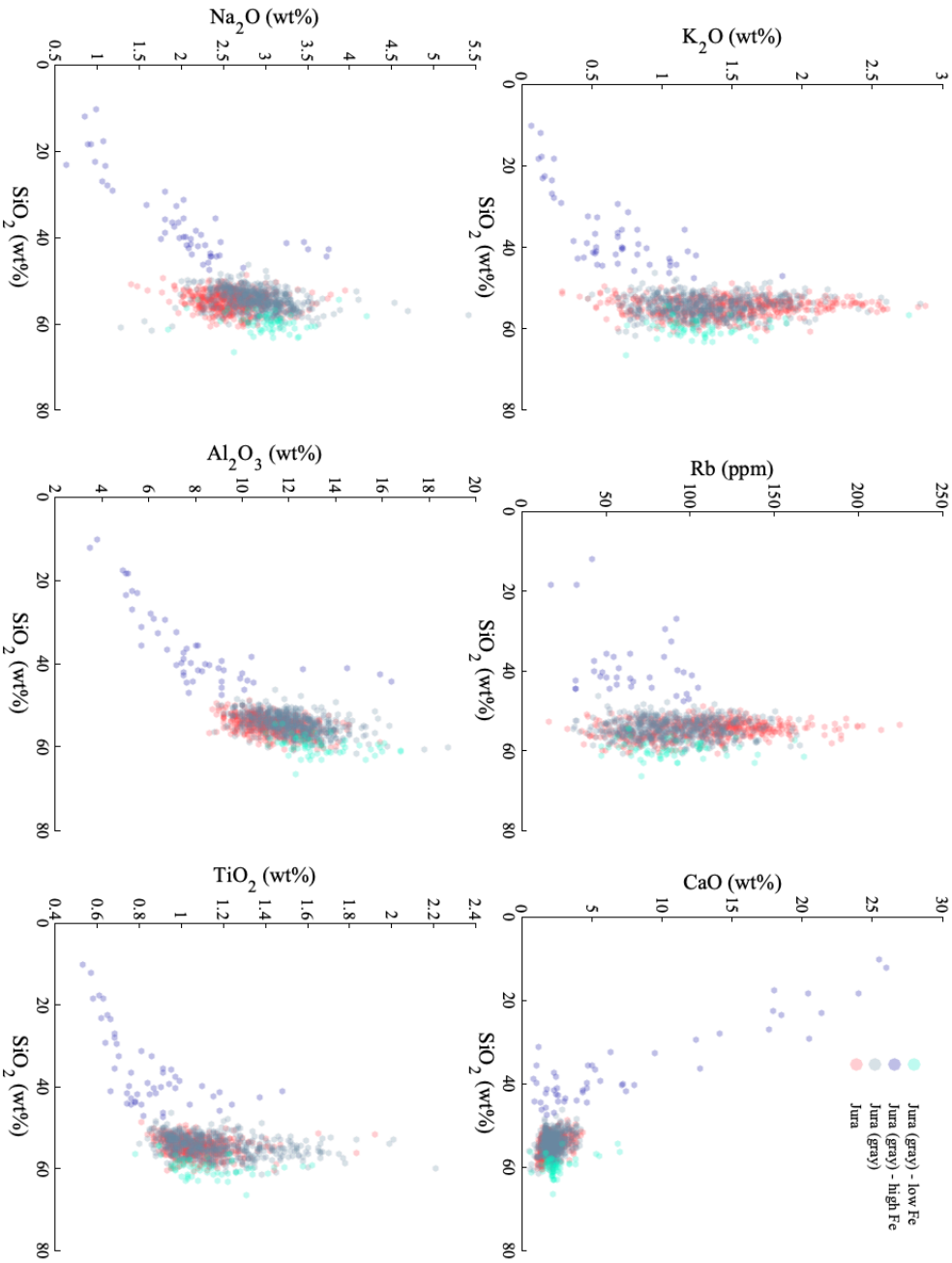

Figure S6. ChemCam observation points on red and gray Jura bedrock, as well as points in gray Jura identified as belonging to the either high or low Fe class. K_2O, Rb, CaO, Na_2O, Al_2O_3, and TiO_2 plotted against SiO_2. Additional high-Fe points exist with FeO_T abundance predicted above 36 wt.%, but they are not included here as they fall outside the predictive range of the ChemCam calibration model.

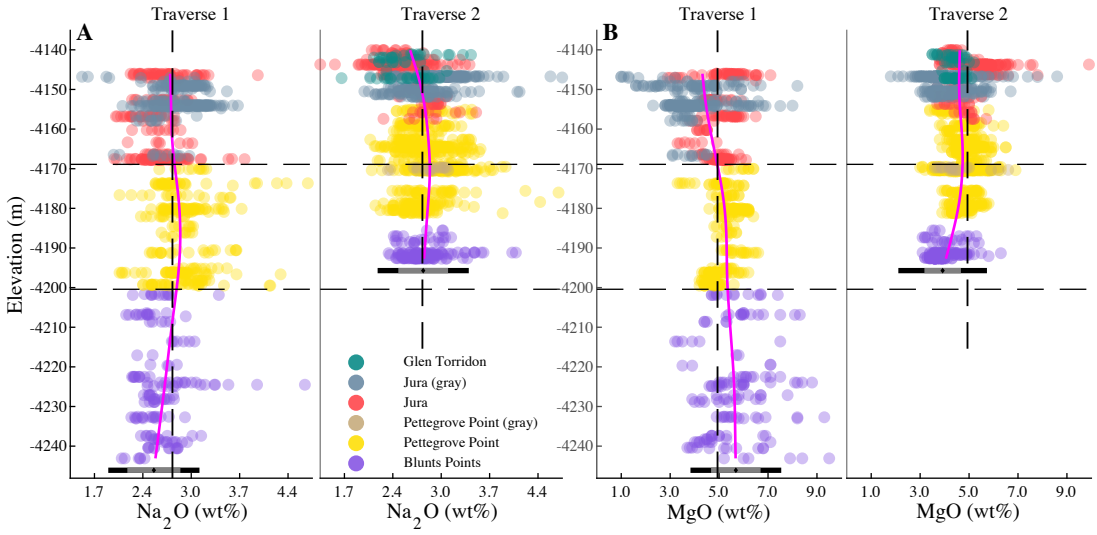

Figure S7. Variations in Na_2O (A) and MgO (B) abundances along the two independent traverses of the ridge from the Blunts Point member below the ridge to Jura at the top of the ridge, including the descent into the Glen Torridon area on the second traverse (Figure 1C). The vertical line represents the mean value on the first traverse, also plotted on the second traverse. Comparably, the horizontal lines represent the contacts between Blunts Point and Pettegrove Point, and Pettegrove Point and Jura members as observed on the first traverse; highlighting how the observed contact between members change in elevation on the ridge. The black bar represents the mean absolute accuracy for all observation points as noted in Table S1; the gray bar rep-resents the relative precision between Murray bedrock targets, see section 3.3 for details. The magenta line is a smoothing spline fitted to the data in each subplot using same parameters as used for the full Murray chemostratigraphy (Figures 3, 4).

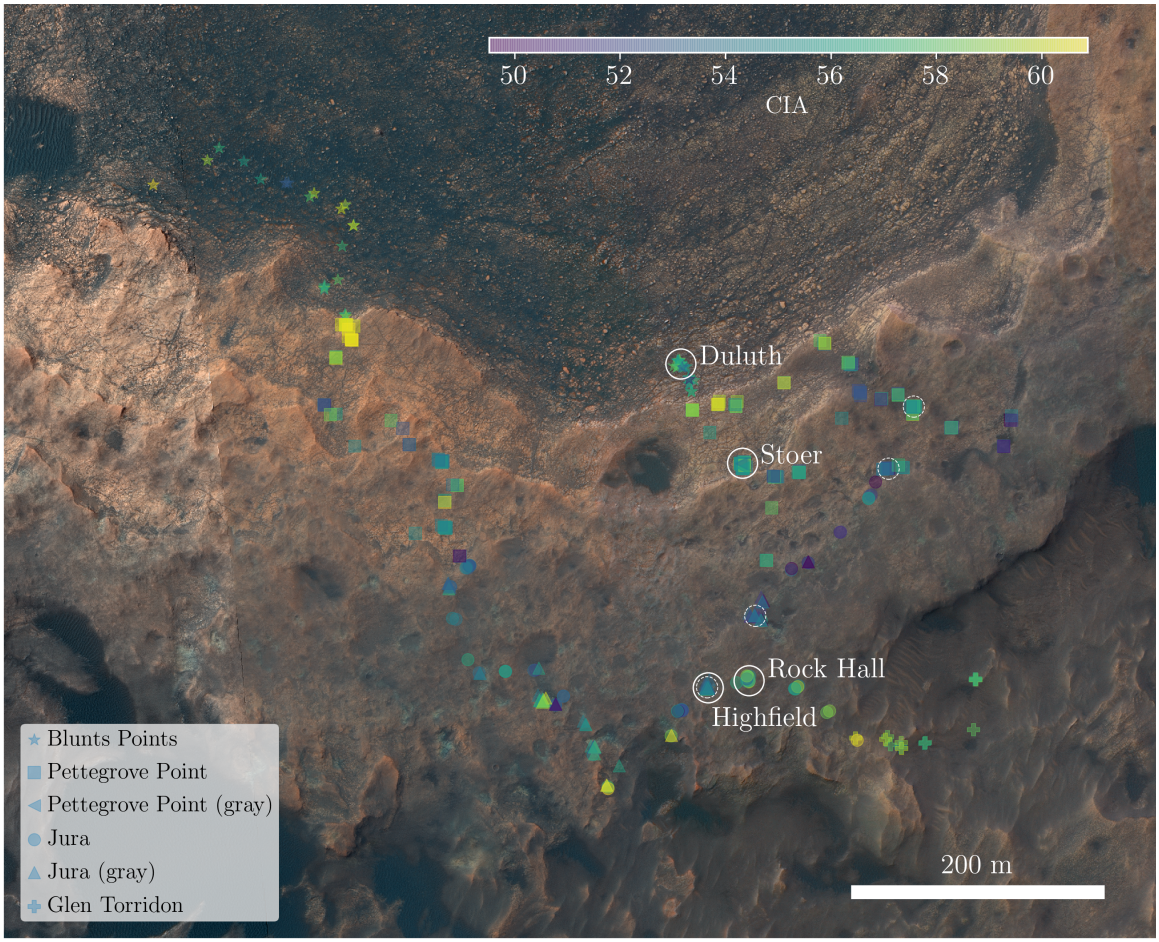

Figure S8. ChemCam observation points plotted on HiRISE mosaic showing the Vera Rubin ridge in Gale crater (Calef & Parker, 2016). Color code indicate the median CIA value of points on bedrock targets in each ChemCam target acquired on the ridge. The location of the four drill sites on VRR is highlighted and named. The location of another four unsuccessful drill sites are annotated with dashed circles.

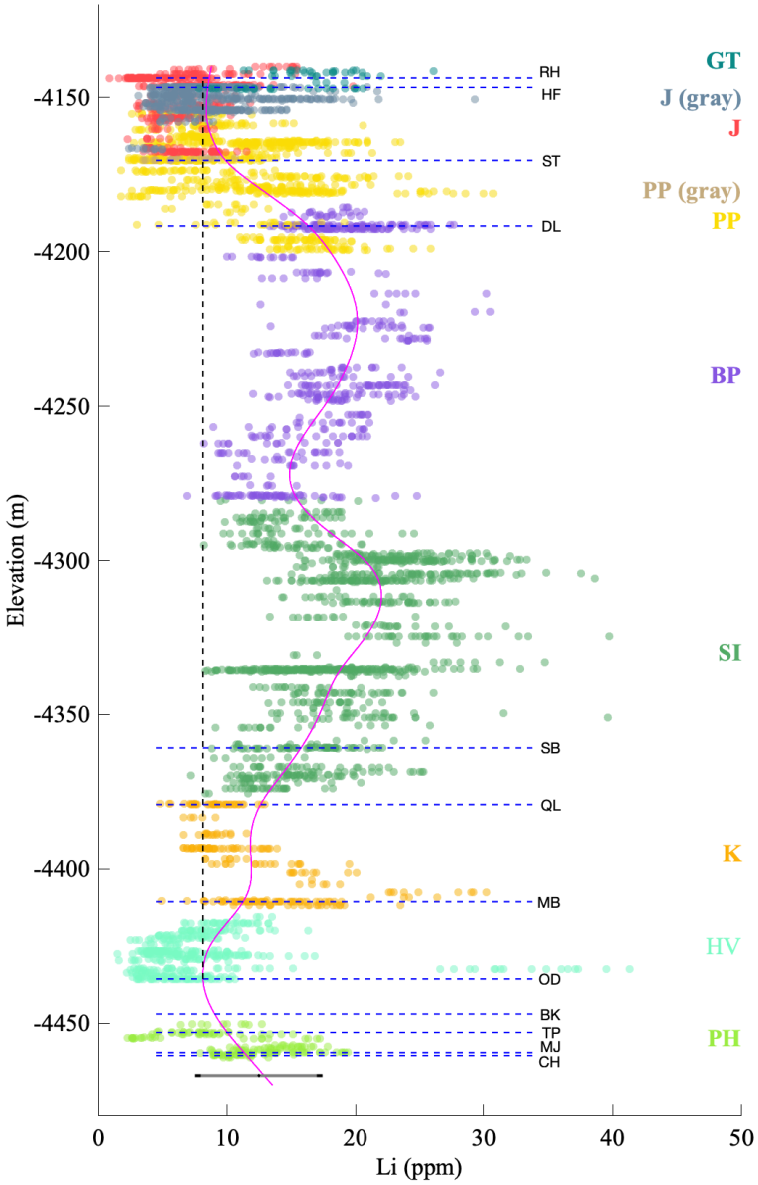

Figure S9. Plotting the Li abundance for ChemCam observation points on Murray Formation rocks against elevation. The black bar represents the mean absolute accuracy for all observation points as noted in Table S1; the gray bar represents the relative precision between Murray bedrock targets, see section 3.3 for details. The magenta line is a smoothing spline fitted to the data in each subplot using same parameters as used for the full Murray chemostratigraphy (Figures 3, 4). The elevation of drill holes in Murray formation rocks have been annotated, and the vertical dashed line projects the abundance (as tracked by the smoothing spline) at the Oudam drill hole up to the elevation of the Highfield drill hole. Drill samples are: CH = Confidence Hill, MJ = Mojave, TP = Telegraph Peak, BK = Buckskin (in Marias Pass class not shown here), OD = Oudam, MB = Marimba, QL = Quela, SB = Sebina, DL = Duluth, ST = Stoer, HF = Highfield, RH = Rock Hall. The annotated classes are: PH = Pahrump Hills, HV = Hartmann's Valley, K = Karasburg, SI = Sutton Island, BP = Blunts Point, PP = Pettegrove Point, J = Jura and GT = Glen Torridon. For J and PP, distinct classes of gray rocks are also annotated. Vera Rubin ridge comprises bedrock from the Pettegrove Point and Jura members.

Table S1 uploaded separately as Excel file

Table S1. All ChemCam geochemistry data included in plots and analyses in the paper. Including which class each point belongs to, the coordinates for the observation point in Gale crater, Mars and the sol the observation was acquired. The 'RMSEP' reflects the model accuracy as detailed in (Clegg et al., 2017), the 'Shots stdev' reflects the standard deviation across number of shots in each point (excluding the first 5 shots). The delta Li and delta Rb reflect the associated uncertainty of the noted abundance as reflected in (Payré et al., 2017). The spacecraft clock noted for each point represent a unique identifier that enables identification and download of the associated raw and processed spectra from the NASA PDS (http://pds-geosciences.wustl.edu/missions/msl/).

Table S2. Specifying the classes identified and the number of observation points from the Pahrump Hills location and into the Glen Torridon area south of VRR assigned to each class. The first column is included in the present analyses and specified in Table S1. The ubiquitous Ca-sulfate veins and cements is classified as 'Point – Murray – Ca' (or Point–Stimson – Ca), and thus represent the single largest class. Other *singular* point classes are small relative to the number of observation points in Murray formation classes.

Included in Supplementary table S1									
Class	#	Class	#	Class	#	Class	#	Class	#
Murray - Pahrump	237	Point - Murray - Al	4	Outcrop - Pahrump	136	Drilltailings - Alisa Craig	10	Dune - scoop dump	40
Murray - Marias Pass	272	Point - Murray - Ca	2470	Conglomorate - Pahrump	43	Drilltailings - Big_Sky	5	Dune - scuff wall	10
Murray - Hartmanns Valley	465	Point - Murray - Fe	38	Concretion - Pahrump	26	Drilltailings - Buckskin	5	Float	166
Murray - Karasburg	265	Point - Murray - K	2	Concretion - Hartmanns Valley	28	Drilltailings - Confidence Hill	17	Float - Bridger Basin	1
Murray - Sutton Island	1327	Point - Murray - Mg	22	Concretion - Karasburg	17	Drilltailings - Duluth	15	Float - Caprock	34
Murray - Blunts Point	621	Point - Murray - Na	56	Concretion - Sutton Island	17	Drilltailings - Greenhorn	8	Float - VRR	269
Murray - VRR - Pettegrove Point	974	Point - Murray - Ti	4	Concretion - VRR - Pettegrove Point	7	Drilltailings - Highfield	15	Low total oxide (S?) - Murray	229
Murray - VRR - Pettegrove Point (gray)	23	Point - Stimson - Al	32	Concretion - VRR - Jura	9	Drilltailings - Lake Orcadie	19	Low total oxide (S?) - Stimson	92
Murray - VRR - Jura	556	Point - Stimson - Ca	151	Pebbles - Butte feature	21	Drilltailings - Lubango	28	Raised feature - Bagnold	22
Murray - VRR - Jura (gray)	555	Point - Stimson - Fe	22	Pebbles - Murray	45	Drilltailings - Marimba	4	Raised feature - Bridger Basin	15
Glen Torridon area	79	Point - Stimson - Mg	27	Pebbles - VRR	31	Drilltailings - Mojave	7	Raised feature - Murray - Blunts Point	15
Point - Murray - Jura - high Fe	2	Point - Stimson - Ti	5	Brandberg feature	53	Drilltailings - Okonuso	38	Raised feature - Murray - Hartmanns Valley	14
Point - Murray - Jura - low Fe	4	Point - vein - Fe	15	Butte feature	45	Drilltailings - Oudam	6	Raised feature - Murray - Jura	6
Point - Murray - Jura (gray) - high Fe	108	Point - Float - Ca	4	Soil	650	Drilltailings - Quela	5	Raised feature - Murray - Pettegrove Point	48
Point - Murray - Jura (gray) - low Fe	61	Point - Murray - Pettegrove Point (gray) - high Fe	1	Dark layer - Murray	137	Drilltailings - Rock_Hall	20	Raised feature - Murray - Sutton Island	24
		Stimson - Marias Pass	594	Dark vein	10	Drilltailings - Stoer	33	Raised feature - Naukluft	23
		Stimson - Naukluft	574	Vein halo - Sutton Island	57	Drilltailings - Telegraph Peak	3	Raised feature - Pahrump	91
		Meteorite	69	Mixed	343				

	Si	K	Rb	Fe	Ca	Na	Al	Ti	Mg	Mn	Li	CIA
Si		0.802	0.633	0.351	-0.36	0.359	0.126	0.45	-0.57	-0.61	0.2	0.1
K	0.802		0.76	0.619	-0.21	0.558	0.105	0.479	-0.72	-0.52	-0.12	-0.19
Rb	0.633	0.76		0.776	-0.63	0.014	-0.12	-0.04	-0.29	-0.42	0.235	0.335
Fe	0.351	0.619	0.776		-0.51	-0.05	-0.21	-0.06	-0.13	-0.02	-0	0.241
Ca	-0.36	-0.21	-0.63	-0.51		0.651	0.615	0.509	-0.45	-0.14	-0.56	-0.83
Na	0.359	0.558	0.014	-0.05	0.651		0.641	0.752	-0.9	-0.49	-0.49	-0.79
Al	0.126	0.105	-0.12	-0.21	0.615	0.641		0.461	-0.56	-0.44	0.063	-0.31
Ti	0.45	0.479	-0.04	-0.06	0.509	0.752	0.461		-0.83	-0.6	-0.52	-0.65
Mg	-0.57	-0.72	-0.29	-0.13	-0.45	-0.9	-0.56	-0.83		0.757	0.433	0.66
Mn	-0.61	-0.52	-0.42	-0.02	-0.14	-0.49	-0.44	-0.6	0.757		0.054	0.249
Li	0.2	-0.12	0.235	-0	-0.56	-0.49	0.063	-0.52	0.433	0.054		0.827
CIA	0.1	-0.19	0.335	0.241	-0.83	-0.79	-0.31	-0.65	0.66	0.249	0.827	

Table S3. Correlation coefficients between smoothing splines fitted to each element plotted in Figures 3 and 4. The 15% highest and lowest correlation coefficients are highlighted in green and red, respectively, to highlight the strongest positive and negative correlations. Importantly, this table does not hold information on point-to-point correlations, only the stratigraphic correlation.